Design and Analysis of a Jet Stretcher for High-Altitude Supersonic Free Jet Testing

Brian C. Heberling* and May-Fun Liou†
NASA Glenn Research Center, Cleveland, Ohio, 44135

Heath H. Reising‡
HX5 LLC, NASA Glenn Research Center, Cleveland, Ohio, 44135

A jet stretcher can be used to extend the region of clean flow for a test article in a supersonic free jet. The device acts to shield the article from shock waves reflected from the free jet shear layer. It can also allow for overexpanded nozzle operation through blocking shocks emanating from the nozzle lip, enlarging the potential test envelope. The FUN3D computational fluid dynamics solver was used to test a design process for developing jet stretchers. The inner surface of the axisymmetric jet stretcher was obtained from a streamline extracted from a free flight simulation around a notional test article at the intended test condition of Mach 3.2, 53,000 ft. The test article and jet stretcher were then simulated in a free jet nozzle exhaust, and the flowfield within a notional inlet aperture was compared between the installed and free flight calculations. Ambient pressure was increased until separation within the free jet nozzle finally induced disturbances at the inlet. The jet stretcher was shown to provide clean flow to the inlet at cell pressure ratios up to 2.8. A process for trimming the axisymmetric jet stretcher was also tested. This was intended to provide blockage relief for complex test articles, aiding with starting, as well as reducing weight and fabrication cost. The trimmed jet stretcher performed identically to the axisymmetric model at slightly-overexpanded conditions, but at cell pressure ratios above 1.3 allowed disturbances from the trailing edge to reach the inlet.

Nomenclature

h	=	Altitude
PR	=	Nozzle exit pressure ratio, $\frac{P_9}{P_1}$
Pt	=	Total pressure
q	=	Dynamic pressure
Tt	=	Total temperature
$y+$	=	Dimensionless wall distance
Subscripts		
0	=	Station 0, nozzle charging station
1	=	Station 1, nozzle exit plane
9	=	Station 9, vacuum tank

I. Introduction

A "jet stretcher" is a device intended to extend the region of clean flow in a free jet. Typically, tests in supersonic flow are limited in axial extent by the "test rhombus" which is bounded on the aft end by the return of waves generated by the test article reflecting from the test section walls (in a wind tunnel) or jet boundary (in a free jet). This is

*Research Aerospace Engineer, Inlets and Nozzles Branch, 21000 Brookpark Rd. M.S. 5-12, AIAA Member
†Research Aerospace Engineer, Inlets and Nozzles Branch, 21000 Brookpark Rd. M.S. 5-12, AIAA Senior Member
‡Research Aerospace Engineer, Inlets and Nozzles Branch, 21000 Brookpark Rd. M.S. 5-12, AIAA Senior Member

especially problematic for air-breathing vehicle models where the propulsion system inlet is located far downstream of the nose. The jet stretcher inner mold line is aerodynamically tailored to the test article to match a streamsurface from the flowfield that would occur in free flight just aft of the bow shock from the forebody. Thus, with knowledge of the free-flight flowfield (made possible by computational fluid dynamics) and accurate positioning, reflections from the free jet boundary are canceled by the jet stretcher external surface.

The earliest report on a working jet stretcher apparatus was presented by R.C. German in 1970[1]. This report identifies the importance of a high-quality nozzle design, as early jet stretcher iterations failed due to non-uniformity in the Mach number and flow angle generated within the nozzle. The accuracy of the as-built jet stretcher to the design contour is also emphasized as prior testing showed inconclusive results due to variances in the fabricated part of up to 0.019". In this test, a jet stretcher design was generated for use in an 8" diameter Mach 3.04 free jet on a von Kármán slender body. Both the jet stretcher axial position and the model angle of attack were able to be remotely positioned during the test. The jet stretcher was demonstrated to be able to provide flow conditions within an acceptable range (local Mach number within ±0.05 and flow angle within ±0.05°) at zero angle of attack on a simulated inlet plane 5 diameters downstream of the model nose. This result was found despite small misalignment and out-of-roundness in the jet stretcher. The test also investigated using this jet stretcher at off-design conditions by changing the jet Mach number and model angle of attack, but found limited success. German[1] references prior work in the mid 1960's by Marquardt Corporation and researchers at Wright-Patterson AFB in developing the jet stretcher concept, but copies of those reports could not be obtained. Jet stretcher development continued at AEDC over the next decade[2,3], but recent examples are absent from the open literature. A common flaw in jet stretcher design methods mentioned in prior reports is the inability to obtain accurate free flight flowfield information to perform the streamline tracing to generate the jet stretcher contour. Modern CFD packages make this calculation relatively trivial. Additionally, more complex analysis such as correcting for boundary layer thickness growth on flow surfaces can be easily carried out with current tools.

II. Motivation

This work aims to study how the installation of a jet stretcher in the NASA Glenn Research Center (GRC) Propulsion Systems Laboratory Cell 4 (PSL-4)[4] could expand the capability for free jet testing. Beyond simply extending the test volume axially by canceling the model bow wave reflection, the facility operating envelope can be extended significantly if the jet stretcher allows for operation of the nozzle at relatively high levels of over-expansion by shielding the model from shock waves emanating from the nozzle lip. Previous free jet tests have used cylindrical shrouds to operate at up to $PR = 2.98$ at Mach 4[5] and $PR = 2.8$ at Mach 5[6].

The typical operating envelope for a 36" diameter free jet nozzle in PSL-4 without a jet stretcher is shown as the region between the $PR = 1$ curve in Fig. 1 and the lower altitude limit presented as the black line. The lower altitude limit is defined by the amount of compressed air supply available to the facility from the Central Air Equipment Building below Mach 3 and the flow rate capability of the J-57 heater engines above. The upper bound is defined by the capability of the central air altitude exhaust system. Because nozzle size is the driving factor in the amount of air being processed by both the supply and exhaust systems, these limits will vary depending on the installation. A 36" diameter was selected as a representative scale for models to be installed within blockage limitations. The increase in capability with at different levels of over-expansion made possible with the jet stretcher is also presented in Fig. 1. It is important to note that each of these curves assumed that the facility spray cooler would be required to cool the exhaust flow due to the heat added by the combustion within the propulsion system model. If the spray cooler is not required, the high-altitude limitation is relaxed significantly below M2.8.

The primary objective of this investigation is to develop a procedure for constructing jet stretcher geometries for a given model profile. This design technique leans heavily on CFD modeling to compute the free-flight flowfield around the model which is required for generating the streamsurface which defines the inner mold line of the jet stretcher. The capability of a representative jet stretcher generated with the technique outlined herein to expand the free jet testing of PSL-4 is also evaluated through CFD. Success of the design technique is evaluated as similarity to the free-flight flowfield at a designated inlet station.

III. Geometry

The simulations examined in this study consist of three components: a free jet nozzle for providing a supersonic freestream flow, a test article, and a jet stretcher. The 36" diameter free jet nozzle was designed using the method of characteristics (MOC)[7] for the desired flight conditions. The contour was corrected for boundary layer displacement through iteration with viscous CFD. The design Mach number used for the MOC was increased based on the displacement thickness predicted at the nozzle exit at relevant Reynolds number conditions. For this design, the inviscid Mach number was 3.25, corresponding to a boundary layer displacement thickness of 0.43" at the nozzle exit.

A notional axisymmetric test article was generated with a length of 175" and a max radius of 9". An inlet face was defined 104" downstream of the nose, consisting of a 90° sector on the bottom of the article with a height of 5". The test article and inlet aperture are shown from profile and forward-looking-aft views in Figures 2 and 3.

The performance of two jet stretchers was investigated. The inner profile of the jet stretchers was defined by tracing a streamline obtained in a free-flight simulation. The streamline was seeded upstream of the nose shock at a radius of approximately 75% of the free jet nozzle radius. The test article is placed within the free jet nozzle such that the nose was 34.5" upstream of the exit plane, allowing the nose shock to pass just downstream of the nozzle lip. The streamline was truncated upstream at the nozzle exit plane and downstream aft of the inlet aperture. The jet stretcher was created by rotationally extruding the streamline into a surface and giving it a thickness of 0.5", with a chamfered leading edge. The radial gap between the jet stretcher leading edge and the nozzle trailing edge is approximately 3.5". The test article and axisymmetric jet stretcher installed in the free jet nozzle is pictured in Figure 4.

A real test article would likely have additional blockage in the form of a physical inlet, control surfaces, and/or fins; making wind tunnel starting a potential concern. Additionally, the axisymmetric jet stretcher is unnecessarily long. It would be desirable to save on weight and material, as well as possibly aid with starting. A "trimmed" jet stretcher was developed from the axisymmetric jet stretcher. Assuming a Mach number within the jet stretcher, a Mach angle can be calculated and used to trim the axisymmetric jet stretcher such that disturbances from the trailing edge will not be able to propagate to the inlet face. This process is depicted in Figure 5. A conservative internal Mach number of 2.5 was used, corresponding with a Mach angle of 23.6°.

IV. Methodology

A. Flow Solution

Simulations were performed using FUN3D version 13.7[8], an unstructured flow solver developed at the NASA Langley Research Center. FUN3D is a node-based, finite volume RANS solver. Simulations assume a calorically perfect gas of single species air. The two-equation Menter Shear Stress Transport (SST) turbulence model[9] using a vorticity source term was used and integrated to the adiabatic walls. All calculations are steady state.

Figure 6 shows the computational domain for the free jet cases. The domain is similar to the PSL-4 test cell, with some simplifications to aid in convergence. The tank is elongated and the entire downstream wall is used as the outflow boundary. The tank is modeled using viscous walls. The free jet nozzle simulations specify a total pressure of Pt_0 = 72.5 psia and total temperature of Tt_0 = 1213.7 °R at the nozzle inflow. A static pressure is applied on the downstream boundary of the computational domain. For each jet stretcher, this pressure is increased until the jet stretcher no longer performs well as judged by the flowfield at the inlet aperture.

The free jet nozzle is intended to provide a Mach number of 3.2 and a dynamic pressure of q = 1500 psf, corresponding with an altitude of approximately h = 53 kft. A simulation of the isolated nozzle predicted conditions of Mach = 3.216 and q = 1489 psf near the nozzle exit where the test article nose was expected to be. These values are used as the freestream boundary conditions for the free flight simulations.

B. Grids

Results from three geometries are discussed in this study: the test article in free flight, the installed axisymmetric jet stretcher, and the installed trimmed jet stretcher. Each grid was uniformly refined until further refinement had a negligible effect on the flowfield at the inlet aperture. Only the grid-converged solutions are discussed here.

Grids were generated using Pointwise version 18.5[10]. Each grid primarily consists of prisms in the boundary layer and tetrahedra elsewhere. Node counts for each mesh are given in Table 1. Initial cell height on all walls is set such that

$y+$ was below unity. Grids are fully three-dimensional and do not take advantage of symmetry.

Table 1. Node counts for each grid.

Configuration	Node Count (millions)
Free Flight	39.3
Axisymmetric Jet Stretcher	113.3
Trimmed Jet Stretcher	141.7

V. Results

A. Free Flight

The test article was first simulated in free flight at conditions identical to those supplied at the exit of the free jet nozzle. Figure 7 presents a contour of Mach number along the symmetry plane. The streamline plotted in black is used for generating the jet stretcher internal surface.

This simulation is also used for validating the performance of the jet stretcher. The goal of the jet stretchers is to maintain a flowfield at the inlet aperture similar to that of free flight. As the free flight simulation is axisymmetric, a radial profile of total pressure is recorded at the station of the notional inlet and will be compared with the jet stretcher simulations.

B. Axisymmetric Jet Stretcher

The axisymmetric jet stretcher was first simulated at slightly-overexpanded conditions of $PR = 1.3$. Mach number along the symmetry plane on the bottom of the test article is shown in Figure 8. The shock from the nose of the test article is positioned correctly in the gap between the jet stretcher leading edge and the nozzle lip. The shock emanating from the nozzle lip is blocked by the jet stretcher.

As the pressure within the test cell increases and the nozzle becomes more highly overexpanded, a boundary layer separation will occur around the nozzle trailing edge. As the cell pressure increases this separation will grow and move upstream, as will the shock. Eventually the shock will move upstream of the jet stretcher leading edge and the jet stretcher will fail to shield the test article.

The test cell pressure was increased until a shock was observed passing upstream of the jet stretcher leading edge. For each simulation, a radial total pressure profile was recorded at the inlet plane and compared with the free flight calculation. Figure 9 presents inlet total pressure profiles for $PR = 2.82, 3.08, 3.33$ against the free flight simulation. For pressure ratios of 2.82 and below, the inlet total pressure closely matched that of the free flight calculation. The jet stretcher flowfield predicted slightly higher total pressure near the edge of the boundary layer.

However, at higher cell pressures the jet stretcher clearly failed. At $PR = 3.08$, there is a drop of 6 psi in total pressure at the inlet face compared with the free flight flowfield. At $PR = 3.33$ the drop is more severe. Figures 10 and 11 show the flowfield near the nozzle exit immediately before ($PR = 2.82$) and after ($PR = 3.08$) jet stretcher failure, respectively. In Figure 10 a large separation exists at the nozzle trailing edge, pushing the shock upstream to the leading edge of the jet stretcher. At this condition, the jet stretcher is barely shielding the test article. In Figure 11 the separation has grown further and the shock has passed upstream of the jet stretcher leading edge, causing the large drop in total pressure at the inlet face. If allowed by the test article geometry, the operating envelope could likely be extended to more highly overexpanded conditions by using a streamsurface closer to the test article for the jet stretcher inner surface.

C. Trimmed Jet Stretcher

The trimmed jet stretcher was developed to reduce weight and material, as well as potentially aid with starting for a more complex test article. The trimming technique using Mach cones should provide an efficient method of removing material with a single design parameter: the Mach angle. For an ideally expanded nozzle, it should provide the same inlet flowfield as the long axisymmetric jet stretcher. However, as the test cell pressure increases from $PR = 1.0$ shocks

will form at the trimmed trailing edge of the jet stretcher. The angle of the shock will increase with cell pressure, causing the shock impingement to move further upstream on the test article. Thus, an additional failure mode has been introduced.

The axisymmetric jet stretcher fails when overexpansion at the nozzle exit causes a separation to grow and moves the overexpansion shock upstream of the jet stretcher leading edge. It extended downstream past the inlet face such that there was no need to consider the trailing edge. Failure may occur from disturbances at the trailing edge, depending on the Mach angle used to trim the jet stretcher.

The trimmed jet stretcher was first simulated at a tank pressure ratio of 1.3, where the nozzle is only slightly overexpanded. Figure 12 shows a symmetry plane Mach contour at this condition, with the inlet plane denoted with a black line. On the bottom of the test article, a shock can be seen passing just underneath the inlet face and reflecting off the test article aft of the inlet. On the top of the test article, where the jet stretcher is much shorter, a much stronger disturbance is impinging upon the article upstream of the inlet axial location.

To examine whether the jet stretcher is successfully shielding the inlet, we must now consider the inlet in three dimensions. Figure 13 presents the total pressure profile along the symmetry plane of the inlet face, while Figure 14 examines a side of the inlet aperture. Pressure ratios between 1.3 and 2.3 are plotted. The $PR = 1.3$ profile is identical to the axisymmetric jet stretcher profiles, along both the center and the side of the inlet. At $PR = 1.8$, the symmetry plane profile is identical to the $PR = 1.3$ profile. However, along the side of the inlet there is a total pressure drop in the boundary layer. At this condition, a disturbance is passing through the side of the inlet. At higher pressure ratios the inlet total pressure continues to drop.

As expected, the trimmed trailing edge jet stretcher performed identically to the axisymmetric jet stretcher at perfectly expanded nozzle conditions. However, increasing test cell pressure resulted in shocks formed at the trailing edge passing through the inlet face; greatly reducing the operating envelope of the trimmed jet stretcher compared with the axisymmetric geometry. Extending the trailing edge of the trimmed jet stretcher downstream would allow for operation at higher cell pressures. This could be done by simply adding a uniform extension to the trailing edge, or by choosing a more conservative Mach angle for the trimming operation.

VI. Summary and Conclusions

The FUN3D computational fluid dynamics solver was used to simulate a test article during Mach 3.2, 53 kft flight and use a streamsurface extracted from the solution to generate a jet stretcher, allowing for testing at identical flight conditions on the ground with a free jet. A long, axisymmetric jet stretcher provided flight-like conditions to a fictitious inlet at cell pressure ratios up to 2.82. It would likely be possible to expand this operating envelope to more highly overexpanded conditions by using a streamsurface closer to the test article, if allowed by test article geometry.

A shorter, trimmed jet stretcher was developed from the axisymmetric model by using Mach cones to remove material in regions where disturbances should not be able to propagate to the inlet. A shorter jet stretcher can provide relief from test article blockage to aid in starting as well as save on weight and material cost. The trimmed jet stretcher performed identically to the axisymmetric jet stretcher at slightly-overexpanded conditions, but at cell pressure ratios above 1.3 shocks from the trailing edge of the jet stretcher affected the flowfield at the inlet. The operating envelope could easily be expanded to higher cell pressures by extending the trailing edge downstream. For a complex test article, a balance must be found to ensure the system is able to start while also able to attain the desired test conditions.

A test validating the jet stretcher design process is currently planned for NASA Glenn Research Center's Advanced Nozzle Test Facility. An axisymmetric body will be tested in a free jet with a trimmed jet stretcher, acquiring data at a notional inlet station using a rotating Pitot rake, while cell pressure is increased to the point of jet stretcher failure. After validation of the design process, future computational work will investigate extending the performance of a trimmed jet stretcher, angle-of-attack testing, and jet stretcher design for a non-axisymmetric test article.

Acknowledgments

This work was supported by NASA's Hypersonic Technology Project under the Advanced Air Vehicles Program. Computational resources supporting this work were provided by NASA's High-End Computing Program through the NASA Advanced Supercomputing Division at Ames Research Center.

References

[1] German, R., "Simulation of Supersonic Flow Over a Body of Revolution Using an Axisymmetric Jet Stretcher," Tech. rep., 1970. doi:10.2514/6.2005-848.

[2] Bauer, R. C., Matkins, E. H., Barebo, R. L., and Armstrong, W. C., "A theoretical and experimental study of a jet stretcher system," *Journal of Spacecraft and Rockets*, Vol. 10, No. 6, 1973, pp. 395–405. doi:10.2514/3.61897.

[3] Matz, R. J., and Kraft, E. M., "Investigations of Free-Jet Test Requirements and Techniques with Emphasis on the Adaptable Jet Stretcher," Aedc-tr-80-35, Arnold Engineering Development Center, Arnold Air Force Station, Tennessee, Apr. 1981.

[4] Soeder, R. H., "NASA Lewis Propulsion Systems Laboratory Customer Guide Manual," Tech. Rep. NASA/TM-106569, Aug. 1994. URL `https://ntrs.nasa.gov/api/citations/19950004410/downloads/19950004410.pdf`.

[5] Bauer, R. C., Muse, W. W., and Tinsley, C. R., "Simulation of Flow Approaching the Chin Inlet of a Ramjet Missile," Aedc-tr-74-5, Jul. 1974.

[6] Molloy, J. K., Mackley, E. A., and Keyes, J. W., "Effect of Diffusers, Shrouds, and Mass Injection on the Starting and Operating Characteristics of a Mach 5 Free Jet Tunnel," Nasa tn d-6377, 1971.

[7] Rice, T., "2D and 3D Method of Characteristic Tools for Complex Nozzle Development Final Report," Tech. rep., 2003.

[8] Biedron, R. T., Derlaga, J. M., Gno, P. A., Hammond, D. P., Jones, W. T., Kleb, B., Lee-rausch, E. M., Nielsen, E. J., Park, M. A., Rumsey, C. L., Thomas, J. L., and Wood, W. A., "FUN3D Manual: 13.7," Tech. Rep. NASA/TM-2020-5010139, Nov. 2020. URL `https://ntrs.nasa.gov/search.jsp?R=20180001971`.

[9] Menter, F. R., "Two-Equation Eddy-Viscosity Turbulence Models for Engineering Applications," *AIAA Journal*, Vol. 32, No. 8, 1994, pp. 1598–1605.

[10] *Pointwise, Version 18.5*, Pointwise, Inc., Fort Worth, TX., Nov. 2021.

Figures

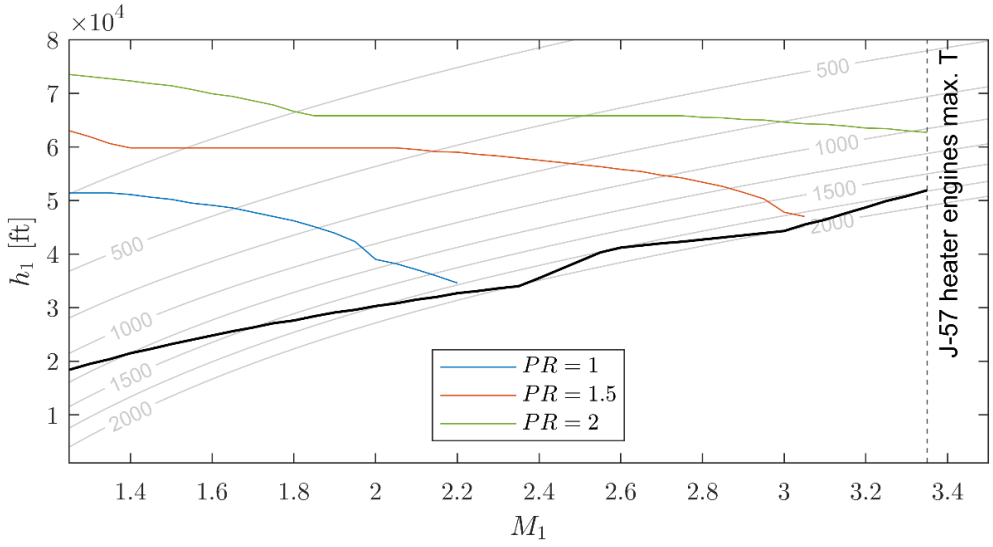


Figure 1. PSL-4 free jet testing capability with a 36" diameter nozzle exit. Lines of constant dynamic pressure are shown in gray for reference and labeled in units of psfa. The lower altitude limit is shown with a black line.

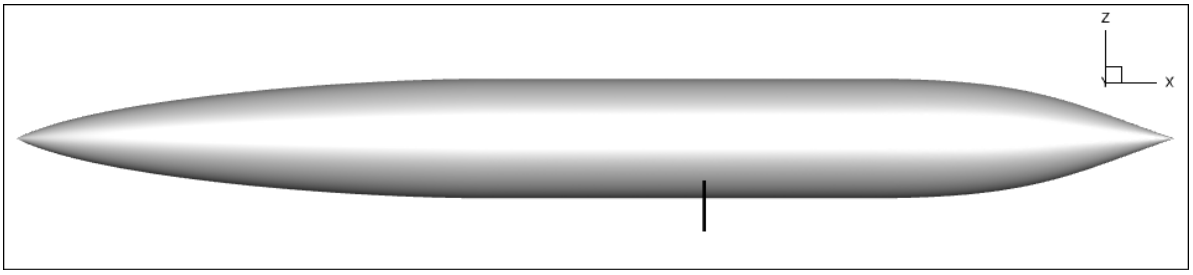


Figure 2. A profile view of the test article, with the inlet aperture shown with a black line. Flow is from left to right.

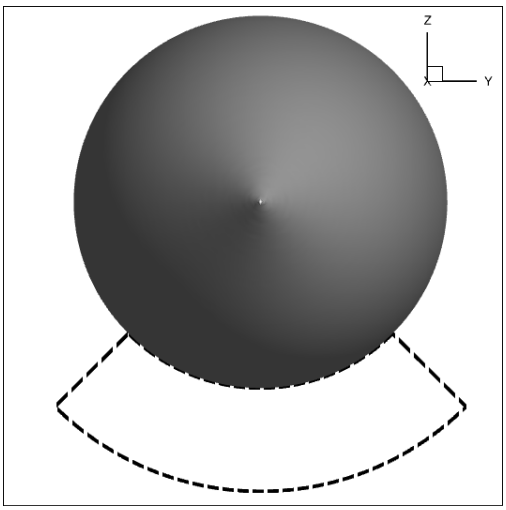


Figure 3. A forward-looking-aft view of the test article with the inlet aperture outlined.

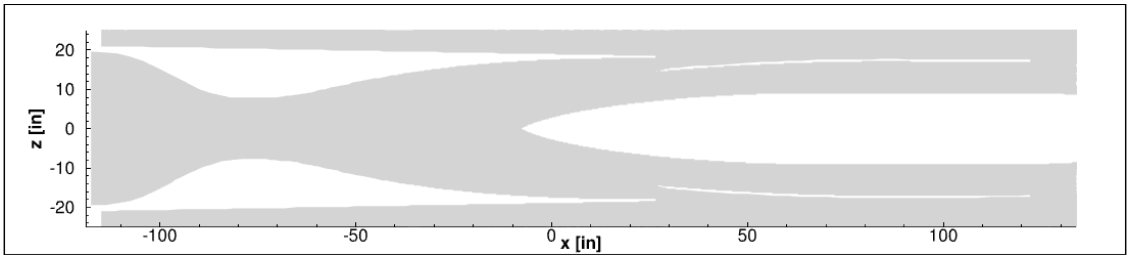


Figure 4. The test article and axisymmetric jet stretcher installed within the free jet nozzle exhaust.

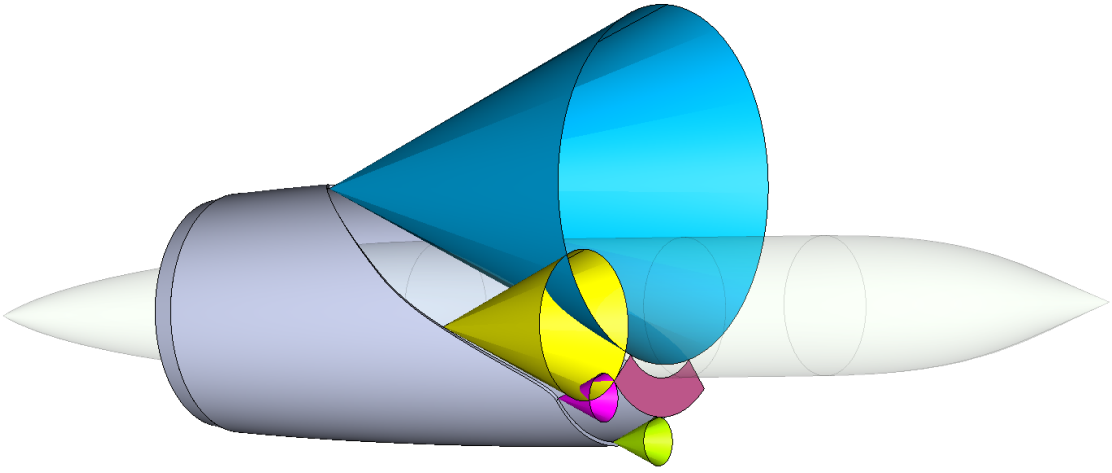


Figure 5. Visualization of the jet stretcher trimming method using Mach cones. The inlet aperture is shown in pink.

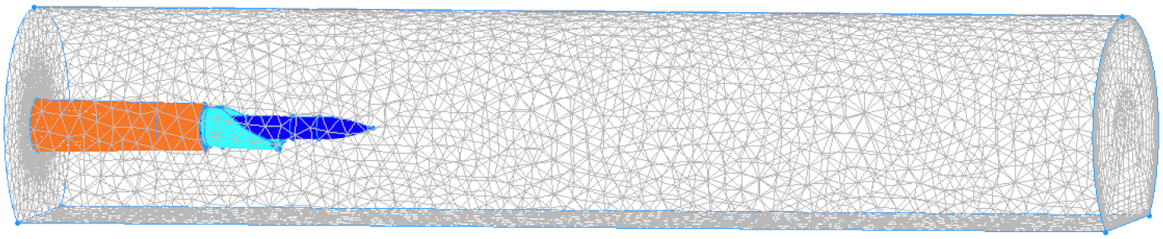


Figure 6. The computational domain for installed simulations. The free jet nozzle in orange, test article in blue, and trimmed jet stretcher in cyan.

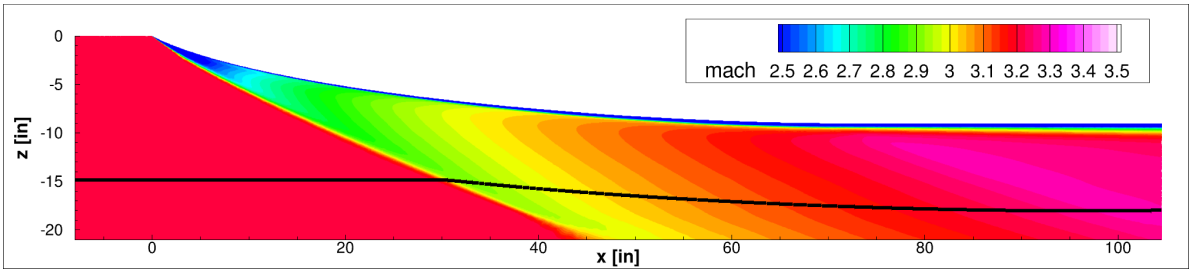


Figure 7. Mach number along the symmetry plane for the free flight test article simulation. The streamline used for generating the jet stretcher inner surface is shown in black.

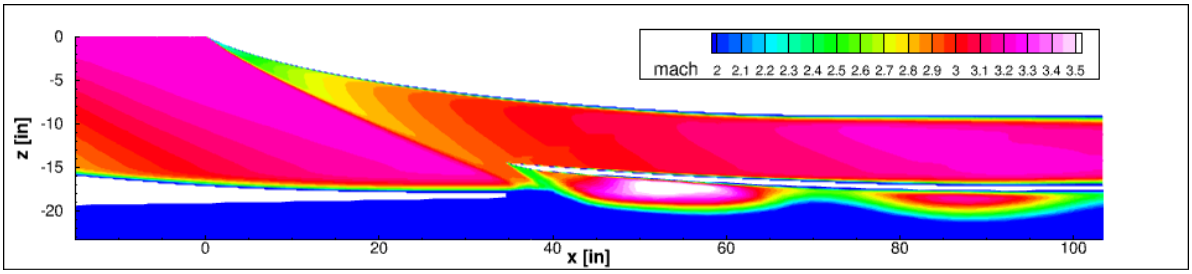


Figure 8. The axisymmetric jet stretcher operating at $PR = 1.3$.

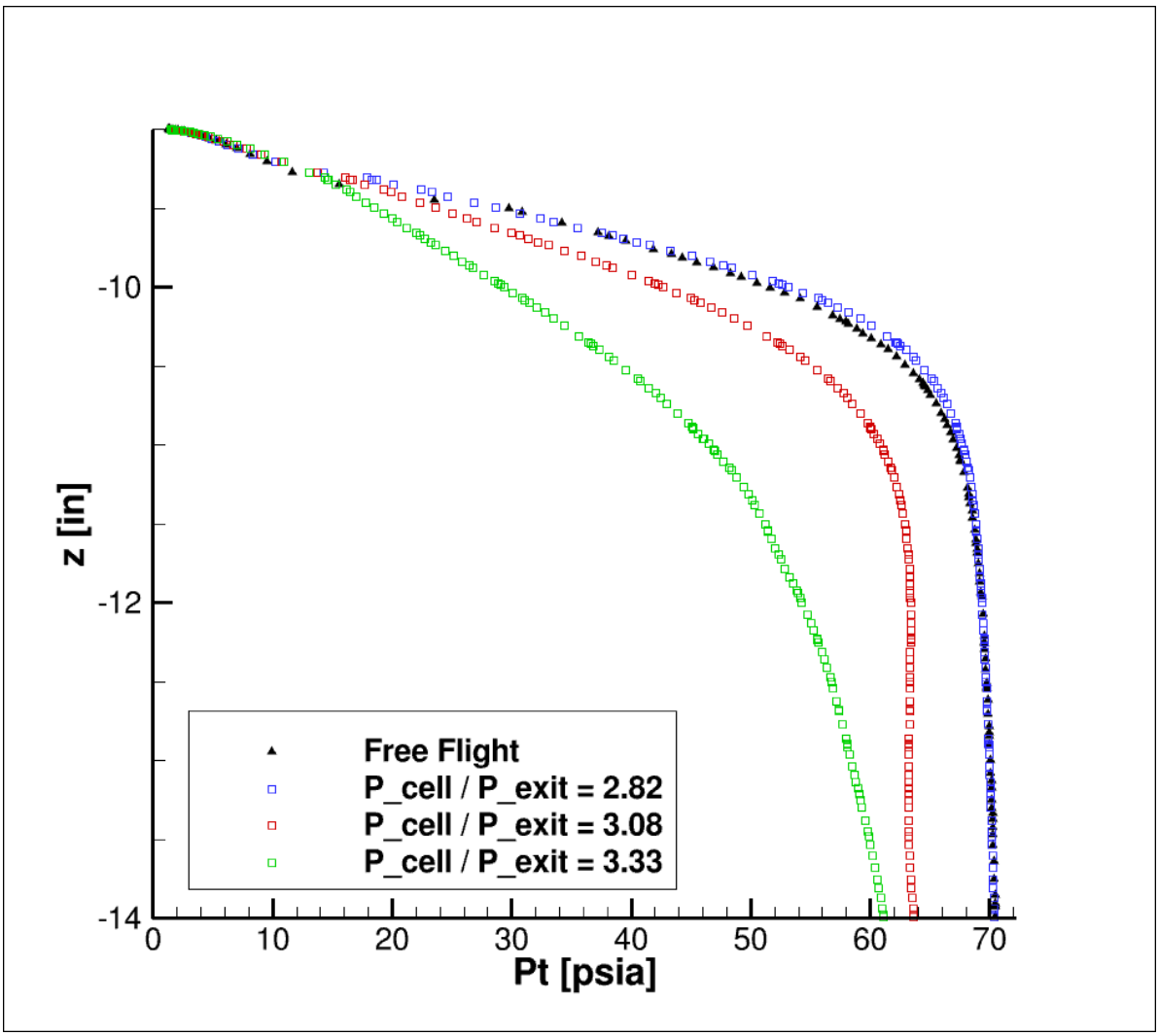


Figure 9. Radial total pressure profiles along the symmetry plane of the inlet for the axisymmetric jet stretcher.

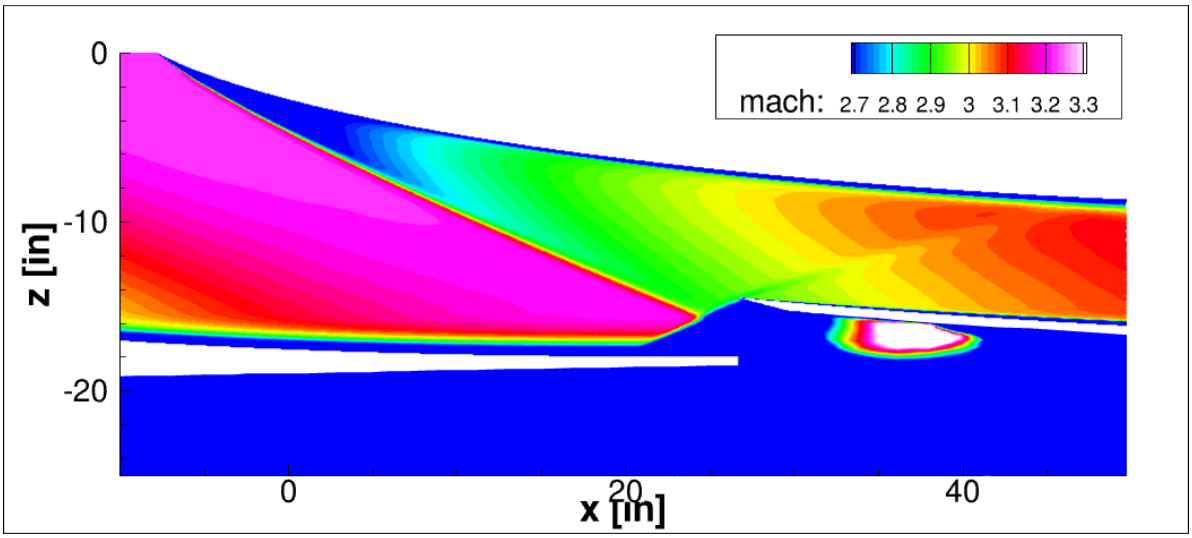


Figure 10. The axisymmetric jet stretcher operating at $PR = 2.82$.

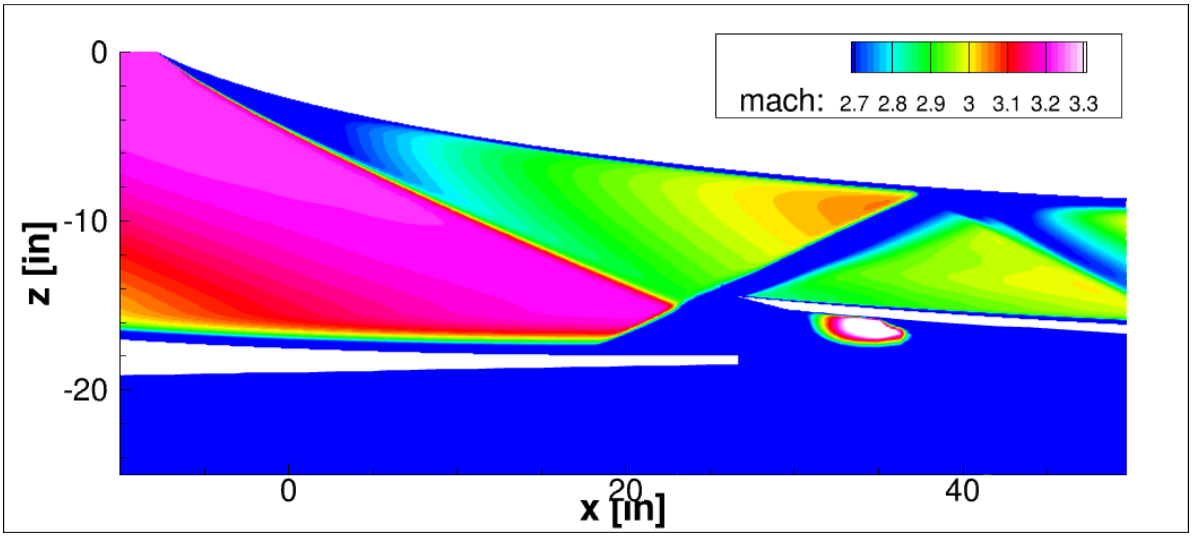


Figure 11. The axisymmetric jet stretcher operating at $PR = 3.02$.

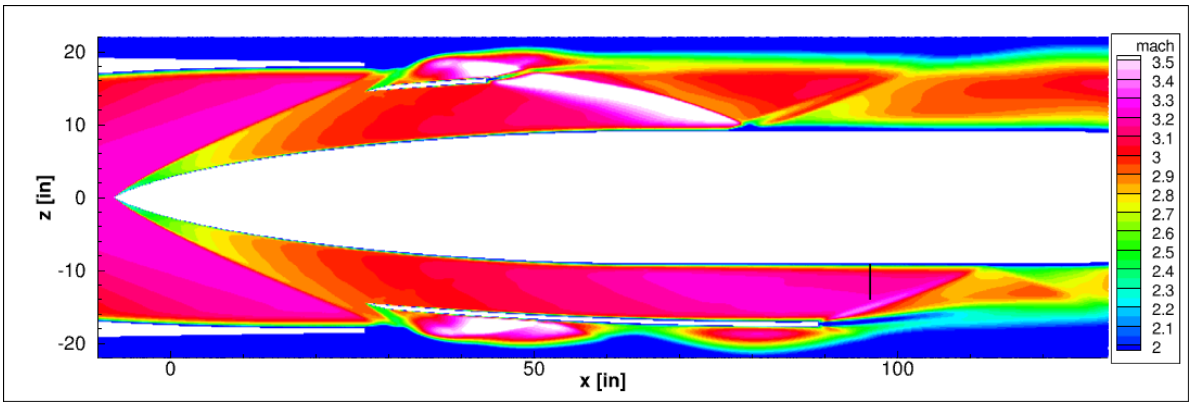


Figure 12. The trimmed jet stretcher operating at $PR = 1.3$.

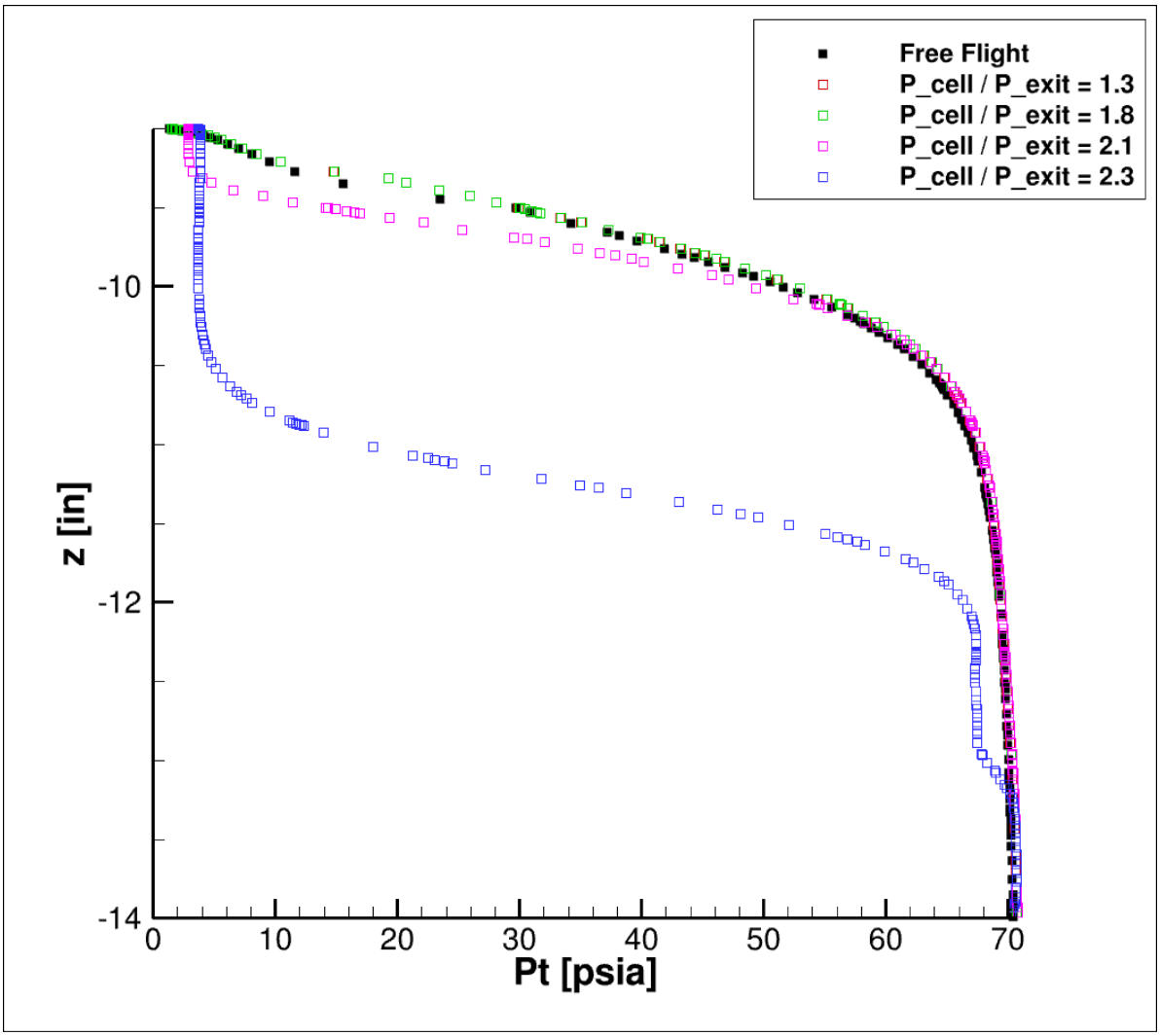


Figure 13. Radial total pressure profiles along the symmetry plane of the inlet for the trimmed jet stretcher.

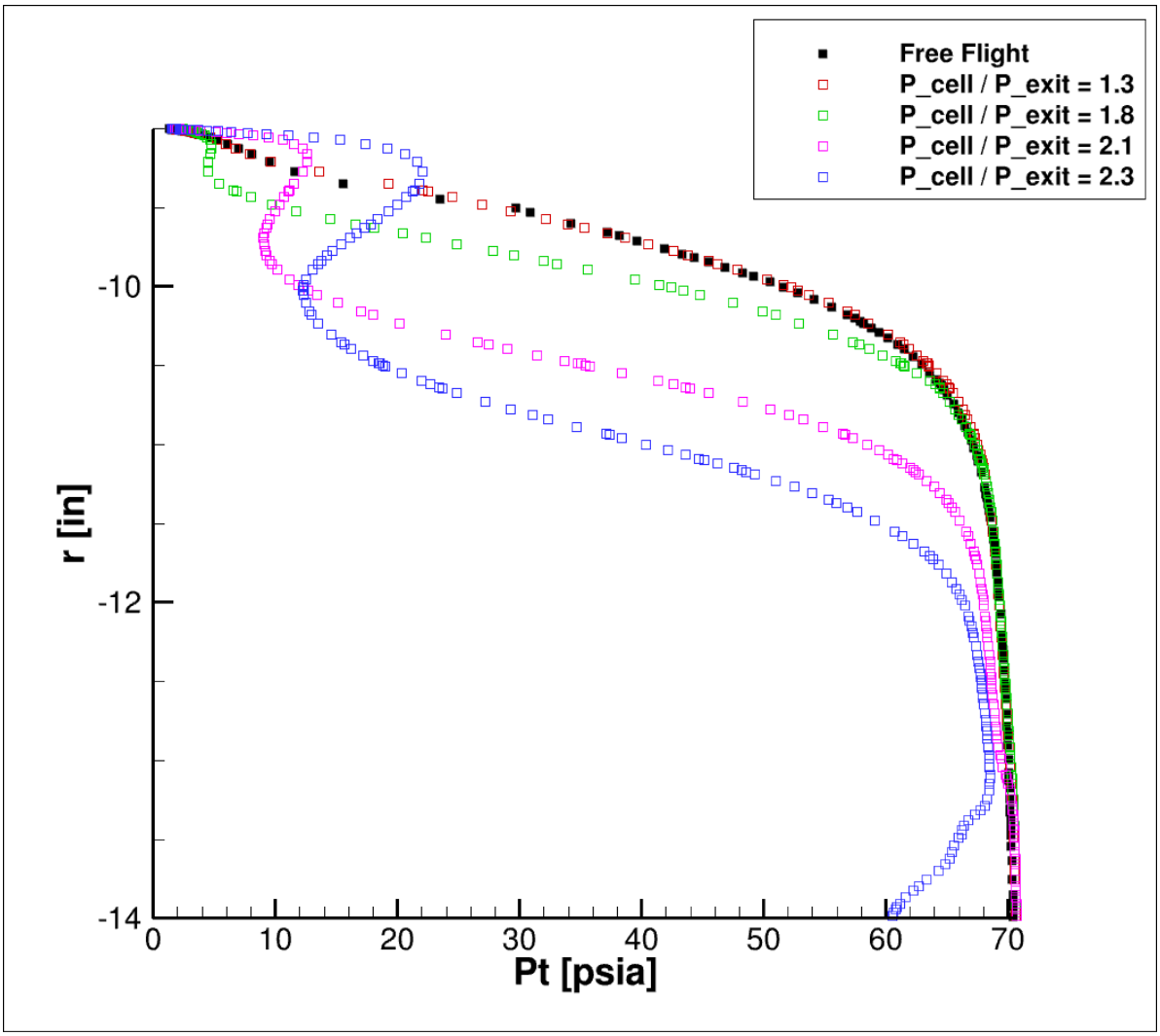


Figure 14. Radial total pressure profiles along the side of the inlet for the trimmed jet stretcher.